NUMERICAL SIMULATION OF AN ALASKA 1964-TYPE TSUNAMI WITH APPLICATION TO BOUNDARY BAY IN THE SOUTHERN STRAIT OF GEORGIA

Isaac Fine, Richard Thomson, and Nicky Hastings

Fisheries and Oceans Canada
Institute of Ocean Sciences
9860 West Saanich Road
Sidney, BC V8L 4B2

2023

Canadian Technical Report of
Hydrography and Ocean Sciences 367

Fisheries and Oceans Canada | Pêches et Océans Canada

Canada

Canadian Technical Report of Hydrography and Ocean Sciences

Technical reports contain scientific and technical information of a type that represents a contribution to existing knowledge, but which is not normally found in the primary literature. The subject matter is generally related to programs and interests of the Oceans and Science sectors of Fisheries and Oceans Canada.

Technical reports may be cited as full publications. The correct citation appears above the abstract of each report. Each report is abstracted in the data base Aquatic Sciences and Fisheries Abstracts.

Technical reports are produced regionally but are numbered nationally. Requests for individual reports will be filled by the issuing establishment listed on the front cover and title page.

Regional and headquarters establishments of Ocean Science and Surveys ceased publication of their various report series as of December 1981. A complete listing of these publications and the last number issued under each title are published in the Canadian Journal of Fisheries and Aquatic Sciences, Volume 38: Index to Publications 1981. The current series began with Report Number 1 in January 1982.

Rapport technique canadien sur l'hydrographie et les sciences océaniques

Les rapports techniques contiennent des renseignements scientifiques et techniques qui constituent une contribution aux connaissances actuelles mais que l'on ne trouve pas normalement dans les revues scientifiques. Le sujet est généralement rattaché aux programmes et intérêts des secteurs des Océans et des Sciences de Pêches et Océans Canada.

Les rapports techniques peuvent être cités comme des publications à part entière. Le titre exact figure au-dessus du résumé de chaque rapport. Les rapports techniques sont résumés dans la base de données Résumés des sciences aquatiques et halieutiques.

Les rapports techniques sont produits à l'échelon régional, mais numérotés à l'échelon national. Les demandes de rapports seront satisfaites par l'établissement auteur dont le nom figure sur la couverture et la page de titre.

Les établissements de l’ancien secteur des Sciences et Levés océaniques dans les régions et à l'administration centrale ont cessé de publier leurs diverses séries de rapports en décembre 1981. Vous trouverez dans l'index des publications du volume 38 du Journal canadien des sciences halieutiques et aquatiques, la liste de ces publications ainsi que le dernier numéro paru dans chaque catégorie. La nouvelle série a commencé avec la publication du rapport numéro 1 en janvier 1982.

Canadian Technical Report of
Hydrography and Ocean Sciences 367

2023

NUMERICAL SIMULATION OF AN ALASKA 1964-TYPE TSUNAMI WITH APPLICATION TO BOUNDARY BAY IN THE SOUTHERN STRAIT OF GEORGIA

Isaac Fine[1], Richard Thomson[1], and Nicky Hastings[2]

[1]Fisheries and Oceans Canada
Institute of Ocean Sciences
9860 West Saanich Road
Sidney, BC V8L 4B2

[2]Natural Resources Canada
Geological Survey of Canada - Pacific Division
605 Robson Street
Vancouver, BC V6B 5J3

Cat. No.: Fs97-18/367E-PDF ISBN 978-0-660-68785-8 ISSN 1488-5417

Correct citation for this publication:

Fine, I., Thomson, R., and Hastings, N., 2023. Numerical simulation of an Alaska 1964-type tsunami with application to Boundary Bay in the southern Strait of Georgia. Can. Tech. Rep. Hydrogr. Ocean Sci. 367: v + 32 p.

CONTENTS

ABSTRACT

Fine, I., Thomson, R., and Hastings, N., 2023. Numerical simulation of an Alaska 1964-type tsunami with application to Boundary Bay in the southern Strait of Georgia. Can. Tech. Rep. Hydrogr. Ocean Sci. 367: v + 32 p.

A high-resolution, nested-grid tsunami model has been used to simulate the distribution of tsunami waves and wave-induced currents that will be generated in Boundary Bay in the event of a magnitude M_w 9.0, 1964-type Alaska earthquake. The model uses an advanced tsunami source distribution and high-resolution bathymetric and topographic data in Boundary Bay. We validated the model by comparing the simulated tsunami waves with those observed during the 1964 event at the Point Atkinson tide gauge. The modelled record closely fits the observed wave forms and amplitudes. According to the model, the tsunami in Boundary Bay will reach 0.45 m above the tidal level at the time the waves arrive, with the first wave being the highest. Tsunami waves along the Semiahmoo coast will be up to 0.35 m. The distribution of tsunami wave amplitudes within Boundary Bay will be non-uniform, with highest waves occurring toward the head of the bay. Moderate strength currents will be induced at the entrance to Drayton Harbor (up to 1.5 m/s) and at the mouth of Campbell River (up to 0.5 m/s). At other locations, wave-induced current will not exceed 0.3 m/s. Even allowing for a 50% safety factor, the risk of flooding in Boundary Bay by an Alaska 1964-type tsunami, is considered to be low.

RÉSUMÉ

Fine, I., Thomson, R., and Hastings, N., 2023. Numerical simulation of an Alaska 1964-type tsunami with application to Boundary Bay in the southern Strait of Georgia. Can. Tech. Rep. Hydrogr. Ocean Sci. 367: v + 32 p.

Un modèle de tsunami à grille imbriquée à haute résolution a été utilisé pour simuler la distribution des vagues de tsunami et des courants induits par les vagues qui seraient générés à Boundary Bay en cas de séisme de magnitude M_w 9,0 de type 1964 en Alaska. Le modèle utilise une distribution avancée des sources de tsunami et des données bathymétriques et topographiques à haute résolution dans Boundary Bay. Nous avons validé le modèle en comparant les vagues de tsunami simulées avec celles observées lors de l'événement de 1964 au marégraphe de Point Atkinson. L'enregistrement modélisé correspond étroitement aux formes et amplitudes d'ondes observées. Selon le modèle, le tsunami à Boundary Bay atteindra 0,45 m au-dessus du niveau de la marée au moment où les vagues arriveront, la première vague étant la plus haute. Les vagues du tsunami le long de la côte de Semiahmoo atteindront 0,35 m. La répartition des amplitudes des vagues du tsunami dans la baie Boundary ne sera pas uniforme, les vagues les plus élevées se produisant vers la tête de la baie. Des courants de force modérée seront induits à l'entrée du port de Drayton (jusqu'à 1,5 m/s) et à l'embouchure de Campbell River (jusqu'à 0,5 m/s). À d’autres endroits, le courant induit par les vagues ne dépassera pas 0,3 m/s. Même en tenant compte d'un facteur de sécurité de 50 %, le risque d'inondation à Boundary Bay par un tsunami de type Alaska en 1964 est considéré comme faible.

1. INTRODUCTION

The second strongest instrumentally recorded earthquake in the World Ocean (M_w 9.2) occurred off Alaska on March 28, 1964. The event generated a catastrophic tsunami, the second greatest in the 20th century after the 1960 Chilean tsunami, with maximum wave heights (trough-to-crest water displacements) of 20 m near the earthquake source region. A large number of landslides and submarine landslides were also initiated, resulting in local tsunami waves as high as 70 m (Lander, 1996). The 1964 earthquake, which was the strongest instrumentally recorded earthquake in the North Pacific and second in magnitude only to the M_w 9.5 Chilean earthquake in 1960, occurred in the vicinity of Prince William Sound, leading to widely used name of the "Prince William Sound Earthquake" (Spaeth and Berkman, 1967). Because of the event date (28 March 1964), the earthquake and associated Pacific-wide tsunami are also called the "Good Friday Earthquake and Tsunami".

The Good Friday tsunami was responsible for close to 130 deaths and about million dollars in damage in Alaska, Washington, California and Hawaii (Spaeth and Berkman, 1967; Lander, 1996;

Stephenson *et al*., 2007). Several locations on the coast of British Columbia sustained major damage (Clague *et al*., 2003; Anderson and Gow, 2004; Stephenson *et al*., 2007), with the highest wave ever recorded in Canada occurring at Shields Bay on the west coast of Graham Island (Haida Gwaii). There, a wave crest was reported to be 5.2 m above the spring high water, or 9.8 m above tidal datum. Most of the damage from the tsunami occurred in Port Alberni, where a wave reached 4.2 m above the spring-tide high water (Dunbar *et al*., 1991; Fine *et al*., 2008).

Several numerical models have been constructed to simulate tsunami wave propagation from the 1964 event in the northeast Pacific Ocean (cf. Dunbar *et al*., 1991; Myers and Baptista, 2001). Although these studies were able to simulate the main features of the tsunami impact on the British Columbia Coast, a more detailed analysis based on recent high-resolution bathymetry and a more refined high-resolution source region of the uplift distribution is needed. Because of its exceptional characteristics, the 1964 Alaska tsunami is typically considered as a proxy for a major future tsunami along the Pacific coast of North America (Suleimani *et al*., 2013).

The purpose of this report is to simulate the expected tsunami waves for Boundary Bay in the southern Strait of Georgia., British Columbia that would be generated by an Alaska 1964-type earthquake with moment magnitude $M_w \sim 9.2$.

2. NUMERICAL TSUNAMI MODEL

2.1. MODEL SETUP: NESTED GRID FORMULATION

Accurate numerical simulation of tsunami waves in the rapidly shoaling regions of the west coast of British Columbia requires setting up the model domain as a series of nested grids of ever finer spatial and temporal resolution. The use of nested grids of smaller cell dimensions and time steps makes it possible to resolve tsunami wave configurations as they propagate into the shallow coastal regions. The principal requirements for numerical models using nested grids are as follows:

- Nested grid cell sizes are generally obtained by dividing the initial, large-scale coarse numerical grid by an integer, typically 3 to 5. Integers larger than this can lead to grid interface problems;

- Nested grids are needed in near-coastal areas; the coarse "parent" grid should be of sufficient extent to resolve possible feed-back effects that the nested grid may have on the parent grid during the simulation time;
- A good interface between the inner and outer domains is required to avoid errors and model instability associated with point matching between the different grids. This should allow two-way fluxes without trapping shorter waves at the inner domain boundaries;
- High resolution bathymetry, external forcing and observations are needed for model domain setup, initialization and validation at each domain level; here the nested-grid formulation is similar to that used in well-known tsunami models, TUNAMI and COMCOT (Liu *et al.*, 1998; Imamura, *et al.*, 2006; Fine *et al*., 2018a,b).

Table 1. Parameters of the numerical grids used in the tsunami generation and propagation model. Grid extent is along the *x* (eastward) and *y* (northward) coordinate directions and is presented in degrees (°). Numerical grid cell sizes for Grids 2, 3 and 4 are roughly 270, 60 and 10 m, respectively. Columns 2,3 and 4 are presented as *x, y* values.

Grid No.	Extent (*x, y*) (degrees)	Array (number of grid points)	Cell size (degrees)	Source of data	Processing type
1	34.0, 16.0	1361, 961	0.025, 0.01667	GEBCO 2014 30 arc- seconds gridded data	Filtering and bilinear interpolation
2	6.595, 4.2	1261,1520	0.005, 0.00333	BC 3 arc-sec bathymetric DEM	Filtering and bilinear interpolation
3	0.74, 0.55	811, 889	0.0008333, 0.0005555	BB 1/9 arc second DEM,	Filtering and interpolation
4	0.38, 0.20	2737, 2161	0.000138889, 0.0000925926	BB 1/9 arc second,	Filtering and interpolation

Because of the relatively long periods of the tsunamis generated in the deep-water source regions used in this study, and because of the relatively short propagation times of 2 to 3 hours

between the source region and the Boundary Bay, the dispersion effect is negligible. In this case, high bathymetric resolution is the important factor for modelling wave propagation in the offshore regions.

The present project uses a series of four nested grids for the Alaska tsunami model (Table 1). The choice of model grids takes into account the need for high spatial resolution to accurately resolve the reflection and transformation of the waves and the need for large spatial extent to capture full source area.

2.1.1. Coarse grid (Grid 1)

Grid 1 is the coarsest numerical grid used in the model. This large-scale grid covers the northeast Pacific and encompasses the major source region used in the simulations for the Alaska tsunami (Figure 1). The northeast Pacific is an important tsunami wave generation region through which all offshore tsunamis propagate on their way to coastal British Columbia. The grid was created using the 30 arc-second global bathymetry dataset GEBCO2014 (GEBCO, 2014).

The spatial resolution of the coarse grid is 90 arc-seconds in the east-west (x) direction (spatial scales ranging from 1.4 km to 2.2 km, depending on latitude) and 60 arc-seconds in the north-south (y) direction (1.85 km grid size). The grid is bounded by 46 – 62° N, 156 – 122° W.

2.1.2. Intermediate grid (Grid 2)

Grid 2 covers water surrounding Vancouver Island, British Columbia and the northwest US coast (Figure 2). The location and coverage of the grid was chosen so that it covered all passes into the Strait of Georgia. This intermediate grid is important for simulating wave transformation as the tsunami enters the Salish Sea through Juan de Fuca Strait. This grid is also important for tsunamis penetrating into the Strait of Georgia through narrow straits, capturing the energy exchange between the deeper shelf waters and the much shallower coastal zone.

The grid was created using the British Columbia 3 arc-second bathymetric Digital Elevation Model (DEM), (NOAA, 2017). Grid 2 has a resolution of 18 arc-seconds in the east-west direction and 12 arc-seconds in the north-south direction, corresponding to spatial scales (x, y) of approximately 370 m and 370 m, respectively (Table 1). The grid boundaries span 47.2°– 51.4°N, 129.8° – 122.2°W.

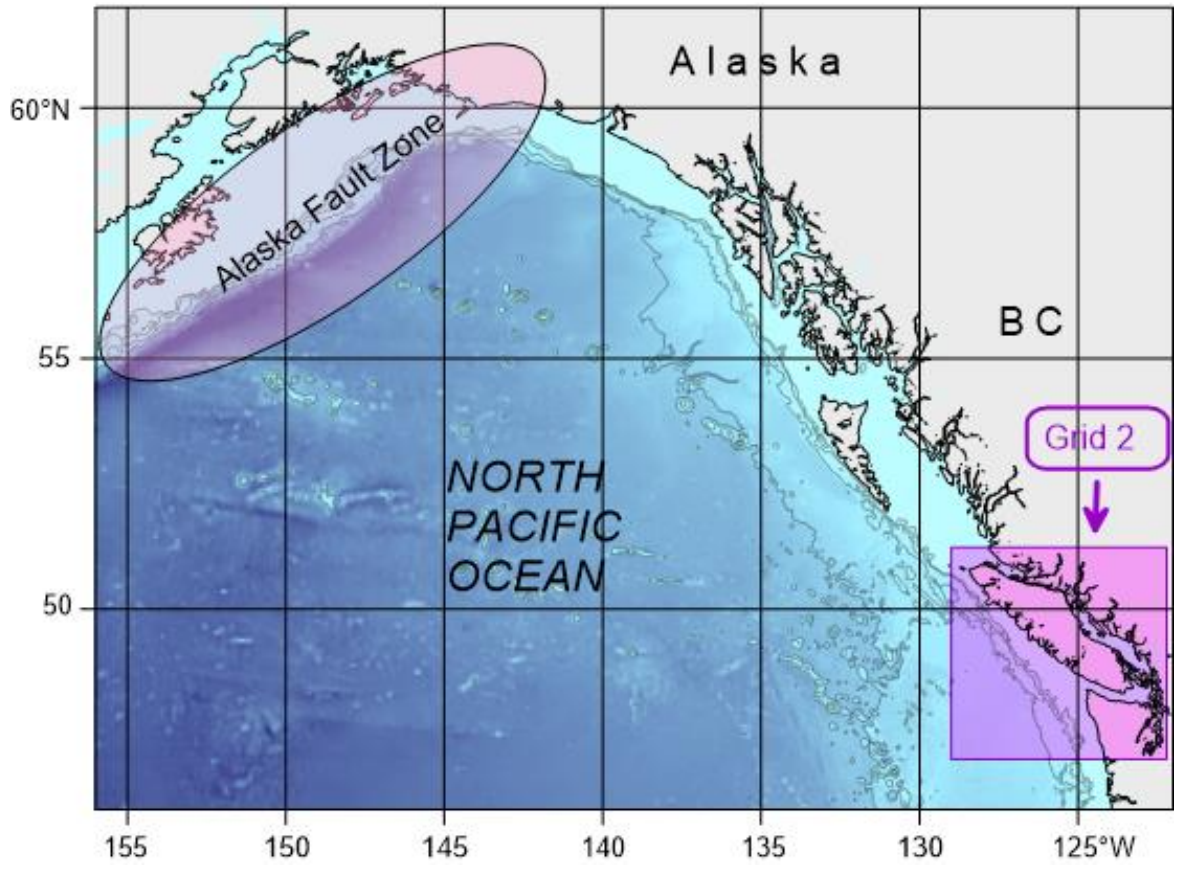

Figure 1. The region covered by the large-scale coarse grid numerical model for the northeast Pacific (Grid 1). Also shown is the Alaska Fault Zone that could generate tsunamis that impact the Boundary Bay. The insert shows the location of the first nested grid (Grid 2), covering the coast of Vancouver Island, British Columbia and northwest Washington State.

To comply with the Grid 3 bathymetry (see Section 1.1.3), we also replaced the Boundary Bay area data of Grid 2 with data computed with a high-resolution digital model for Boundary Bay; the original 3-arc second data in that area are too inaccurate for that region.

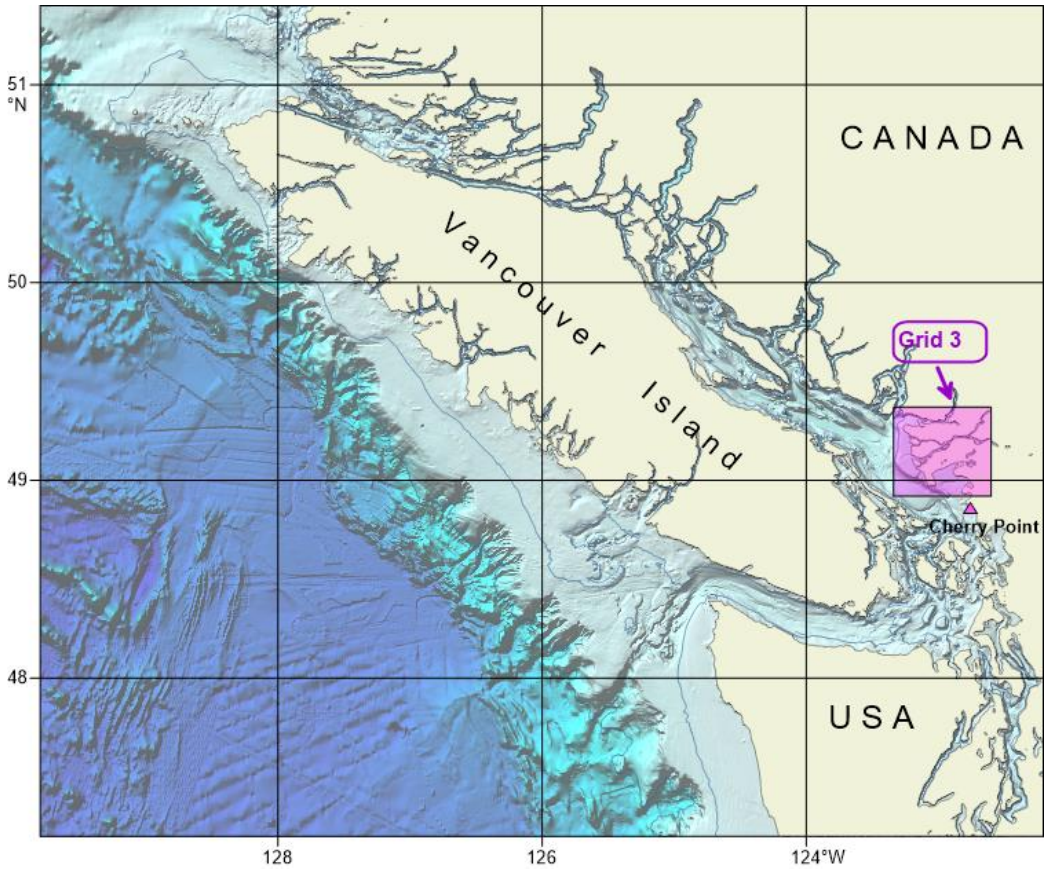

Figure 2. Vancouver Island and surrounding oceanic regions covered by the medium-scale bathymetric grid (Grid 2) for the southwest coast of British Columbia. The horizontal grid cell scales (x, y) for this region are approximately 370 m. The insert shows the boundaries and location of the second nested grid (Grid 3) covering the region of Metro Vancouver and Boundary Bay.

2.1.3. Intermediate grid (Grid 3)

The third numerical grid covers the waters surrounding Metro Vancouver (Figure 3). This grid is of considerable importance because it determines wave transformation in the vicinity of Boundary Bay. Model grid cells were created using the 1/9 arc-second Boundary Bay digital Elevation Model (BBDEM, 2020). The gridded data were subsequently re-interpolated to a geographical coordinate system (NAD83 standard) with a rectangular grid cell size of 3 arc-seconds by 2 arc-seconds (approximately 61 m by 62 m) in the east-west and north-south directions, respectively.

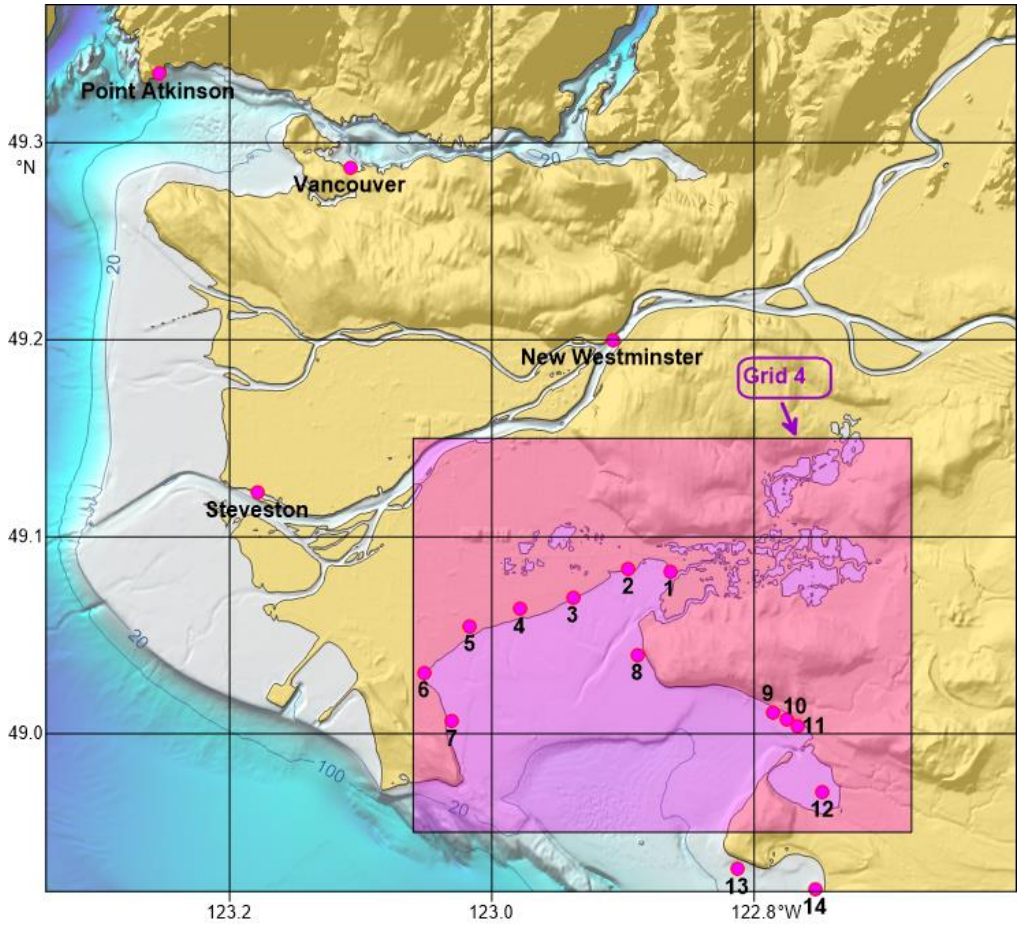

Figure 3. The coastal region covered by Grid 3, including the waters surrounding Greater (Metro) Vancouver. The *x*, *y* grid scales for this region are approximately 61 m and 62 m, respectively. Shown are the locations of the tide gauges (solid dots) and the modelled sites (numbers 1-14). The area above mean sea level is shaded yellow. The insert shows the boundaries and location of the fourth nested grid (Grid 4) covering Boundary Bay.

2.1.4. Final grid (Grid 4)

The final (fourth) numerical grid has the highest spatial resolution of roughly 10 m by 10 m and covers Boundary Bay (Figure 4). The grid has been created specifically for the Boundary Bay area and is designed for estimation of tsunami inundation and tsunami-induced currents.

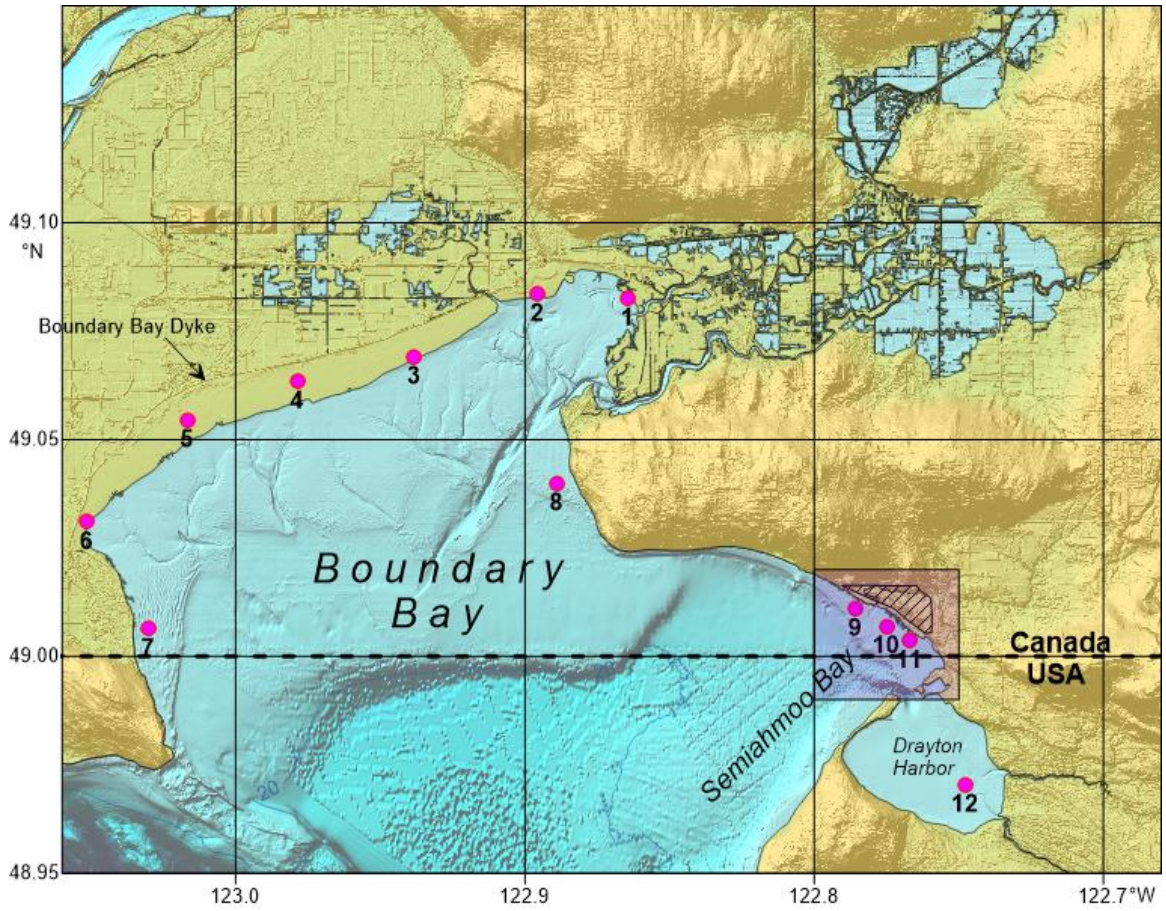

Figure 4. The region covered by Grid 4. The fine-scale bathymetric grid has adjusted topography for Boundary Bay, with grid scales (x, y) of approximately 10 m by 10 m. Also shown are the sites (numbers 1-12) in Boundary Bay for which tsunami wave records have been simulated. Depths, H, are in metres (m). The area above mean sea level is shaded in yellow. The hatched area denotes the location of the Semiahmoo, First Nation Reserve.

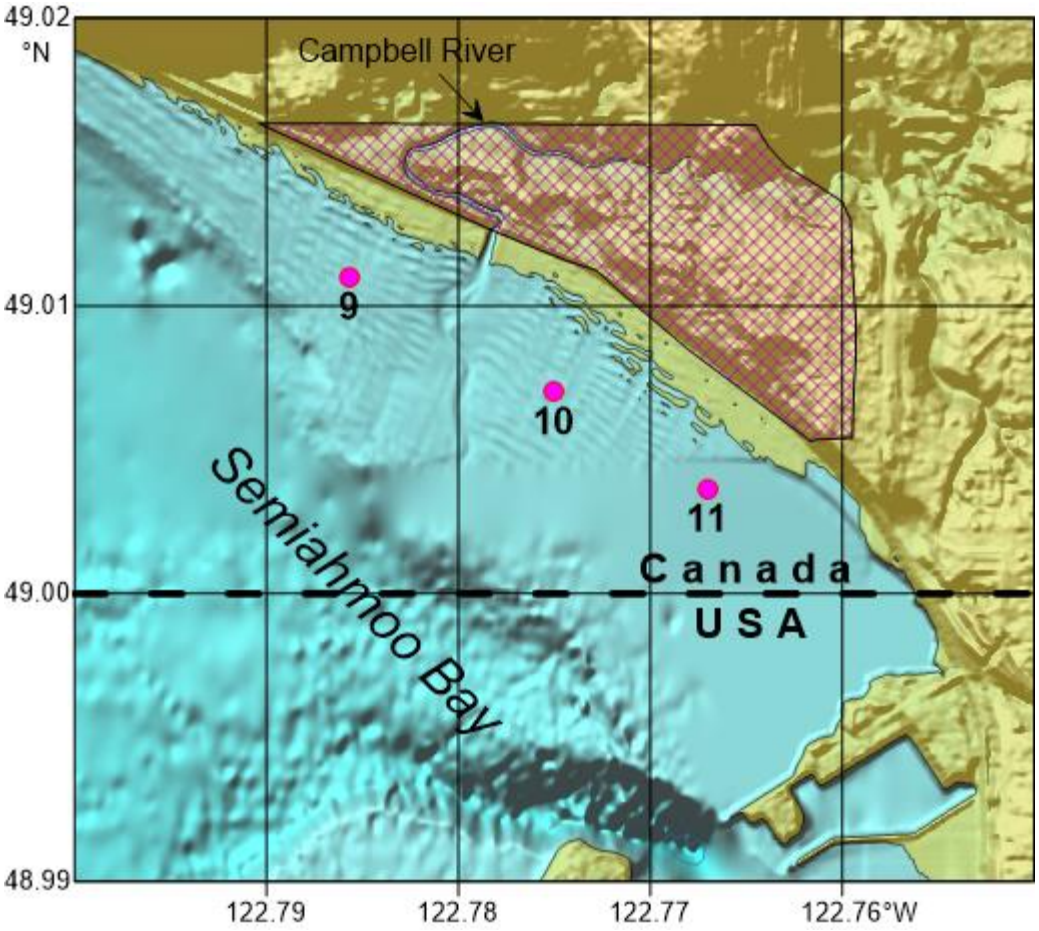

Figure 5. A fragment of the area covered by Grid 4, surrounding the Semiahmoo First Nation Reserve (shaded by a mesh). Also shown are locations of the Sites 9-11 for which tsunami wave records have been simulated. The area above mean sea level is shaded in yellow.

2.2. MODEL REFERENCE LEVEL

Model simulations are generally conducted for tsunami arrival times that coincide with times of Canadian Vertical Datum of higher high water mean tide (HHWMT). The National Tsunami Hazard Mapping Program of 2010 (Nikolsky *et al.*, 2013) recommends that inundation maps be computed using high tide as the initial condition for modelling. Alaska University uses Mean Higher High Water (MHHW) as the initial condition (Suleimani et al., 2013), while Washington State inundation map was created using Mean High Water (MHW) for initial conditions (Eungard *et al.*, 2018. The Canadian standard HHWMT is close to the US standard MHHW, and has been used for many tsunami modelling projects in BC for Victoria (AECOM, 2013) for Victoria and Seal Cove (Fine *et al*., 2018a, 2018b), and for Prince Rupert (The City of Prince Rupert Tsunami Flooding Risk Assessment, 2019). Accordingly, to present values of highest risk, maps of maximum tsunami wave amplitudes and current speed in this report are referenced to HHWMT rather than to the mean tide or to a geodetic reference.

Higher High Water Mean Tide (HHWMT) is used as the primary reference level for most modelling results. For the Boundary Bay area, the closest permanent tide gauges are at Point Atkinson and Vancouver (Canadian Hydrographic Services) to the north and Cherry Point (NOAA) to the south. HHWMT is 1.30 m above Mean Sea Level (MSL) at Point Atkinson and 1.32 m above MSL at Vancouver; in comparison, MHHW used in the US is 1.18 m above MSL at Point Atkinson (see Table 2 below). For convenience, a common reference value of 1.2 m is added throughout the region for the tsunami modelling. Mean Sea Level (MSL) is 0.18-0.19 m above the Canadian geodetic datum CVD2013 (Table 2).

However, when examining the waves themselves, the wave displacement, h, presented in the figures can be considered as the wave crest amplitude (upward water level displacement) measured relative to the tide level at the time of the tsunami arrival. This has a positive value. Sometimes, we want to show the depth of the wave trough, in which case “height” (= downward water level displacement) will have a negative value measured downward from the tide level at the time of the tsunami.

Table 2. Vertical datum values for tidal stations provided by the Canadian Hydrographic Service and NOAA (USA). Latitude and longitude are in degrees and minutes. Mean Higher High Water (MHHW) and Mean Lower Low Water (MLLW) are defined in two ways: (1) in Canada using tidal predictions derived from tide gauge records; and (2) in the United States using observations from USA tide gauges. All values are referenced to Mean Sea Level (MSL), which by definition in this study is then zero (0.0). Here, CGVD 2013 denotes the Canadian Geodetic Vertical Datum.

Tide gauge ID	Name	Latitude (°N)		Longitude (°W)		CGVD 2013	MSL	MHHW	MLLW
		Deg	Min	Deg	Min	(m)	(m)	(m)	(m)
7795	Point Atkinson	49	20.25	123	22.42	-0.193	0.0	1.30	-1.94
7735	Vancouver	49	17.23	123	6.587	-0.18	0.0	1.32	-1.96
9449424	Cherry Point	48	51.8	122	45.5	-	0.0	1.18	-1.61

2.3. THE SOURCE DISTRIBUTION

Numerical simulation of the 1964 tsunami is based on the newly revised (Suleimani *et al*., 2013) coseismic slip distribution for the 1964 rupture founded on the model of Suito and Freymueller (2009). This is a three-dimensional viscoelastic model, in combination with an after-slip model, which uses realistic geometry with a shallow-dipping elastic slab to describe the post-seismic deformation that followed the 1964 earthquake. The authors applied the inversion-based model by Johnson *et al*. (1996) as a basis for their coseismic slip model, adjusting it to the new geometry and critically reinterpreting the coseismic data. Suleimani (2011) used results of the near-field modelling of the 1964 tsunami to constrain the amount of slip placed on intraplate splay faults, and to evaluate the extent of the Patton Bay fault. The revised model includes contributions from coseismic horizontal displacements into the initial tsunami wave field through the component of the ocean surface uplift due to horizontal motion of the steep ocean bottom slopes. The tsunami simulations revealed that including deformation due to horizontal displacements in the source function resulted in an increase in the far-field tsunami amplitudes. The coseismic vertical deformation resulting is shown in Figure 6.

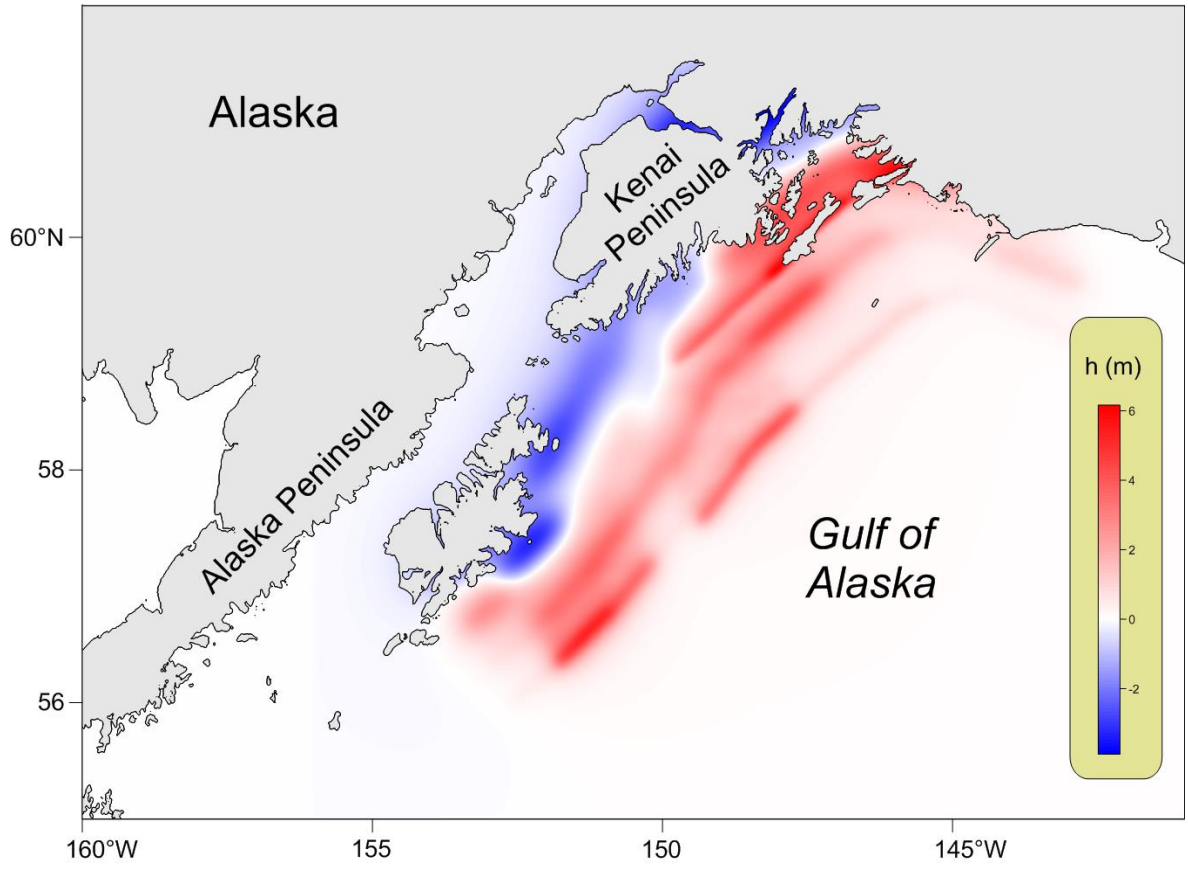

Figure 6. Seafloor vertical displacements (m) at the source region for the March 1964 Alaska tsunami from (Suleimani *et al*., 2013). Seafloor displacements range from roughly -3 m (*blue*) to +6 m (*red*).

3. RESULTS

3.1. COMPARISON WITH THE OBSERVED RECORD AT THE POINT ATKINSON TIDE GAUGE

To verify the model, we compared the modelled results with the record of the Alaska 1964 tsunami at the Point Atkinson tide gauge (Figure 3). The original analogue record of the tsunami was first digitized and the tides then carefully subtracted from the digital record using tidal analysis programs (cf. Thomson and Emery, 2014). In addition, low-frequency oscillations were removed from the observations using a polynomial approximation of the residual sea level.

Comparisons of the observed and modelled results are shown in Figure 7. It is evident that the modelled record fits the observed record quite well. For both the observed and simulated records, the first crest wave is the largest wave. The maximum tsunami travel times coincide within 10 minutes, and phases of the first four waves are close, indicating that the records are very similar, despite the observations being based on a digitized analogue record.

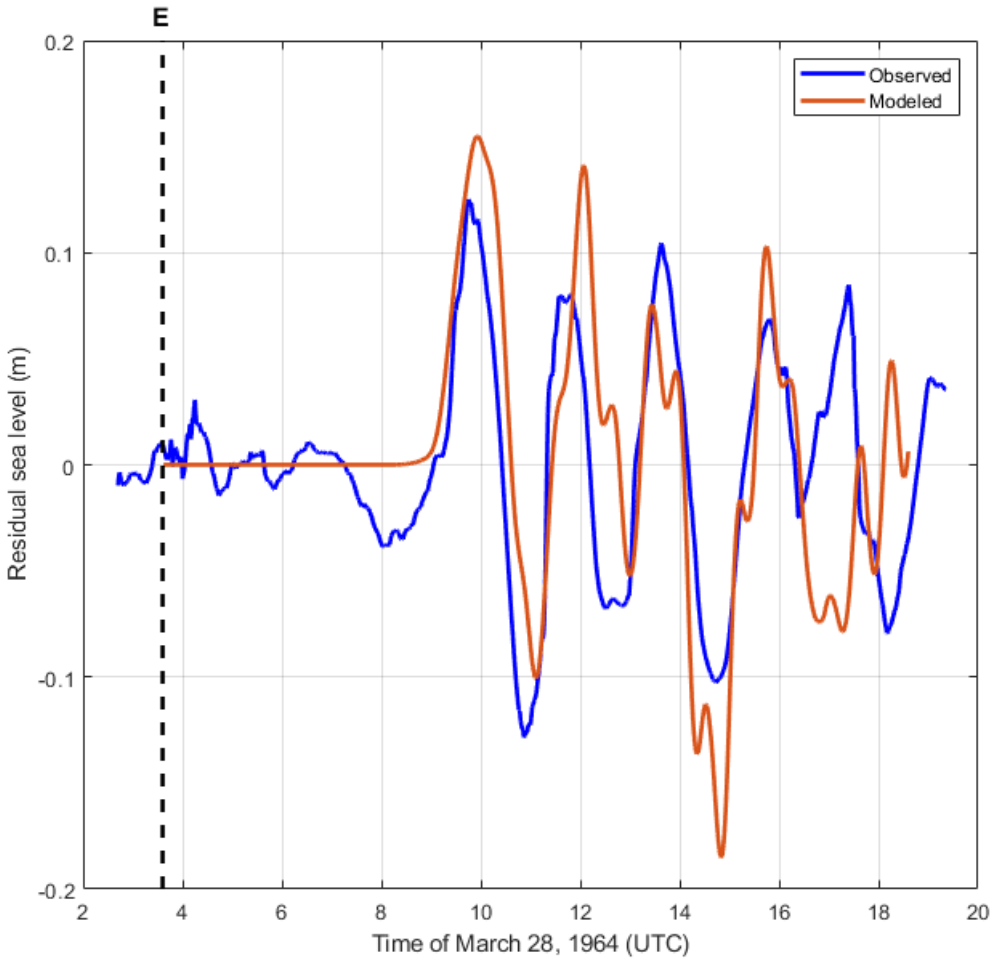

Figure 7. Observed versus modeled wave records for the March 1964 Alaska tsunami for the Point Atkinson tide gauge site. The letter "E" denotes the time of the earthquake.

The maximum wave crest in the modelled record is higher than the maximum of the observed record by 20%, but the trailing trough in the modelled wave train is slightly lower than that in the observed record. As a consequence. the tsunami height (trough-to-crest range) of the first wave is almost the same for the modelled and observed time series. The observational record shows that a small trough preceded the first crest, which is not in the modeled record. In general, comparison of the observed and modeled series demonstrates that the model adequately simulates tsunami waves in even regions, such as the Strait of Georgia, that are sheltered from tsunamis arriving from the open ocean.

3.2. MAXIMUM TSUNAMI WAVE AMPLITUDES

The computed distributions of the maximum wave amplitudes (~½ the crest-to-trough difference in water displacements or "wave heights") for a future Alaska-type tsunami based on grids 1-3 are presented in Figures 8-10. Figure 8 shows the "rays" of maximum tsunami wave amplitudes for the entire northeast Pacific. While tsunami wave-amplitude maxima are found in Prince Williams Sound (the source area), considerable tsunami energy is radiated to the southeast toward the coast of California. In British Columbia and along the US West Coast, the most affected coastal zones are those exposed to the open ocean, such as the west coast of Vancouver Island and the west coast of Washington State. In more protected areas, such as Juan de Fuca Strait, the computed tsunami wave amplitudes are markedly smaller (Figure 9; Grid 2).

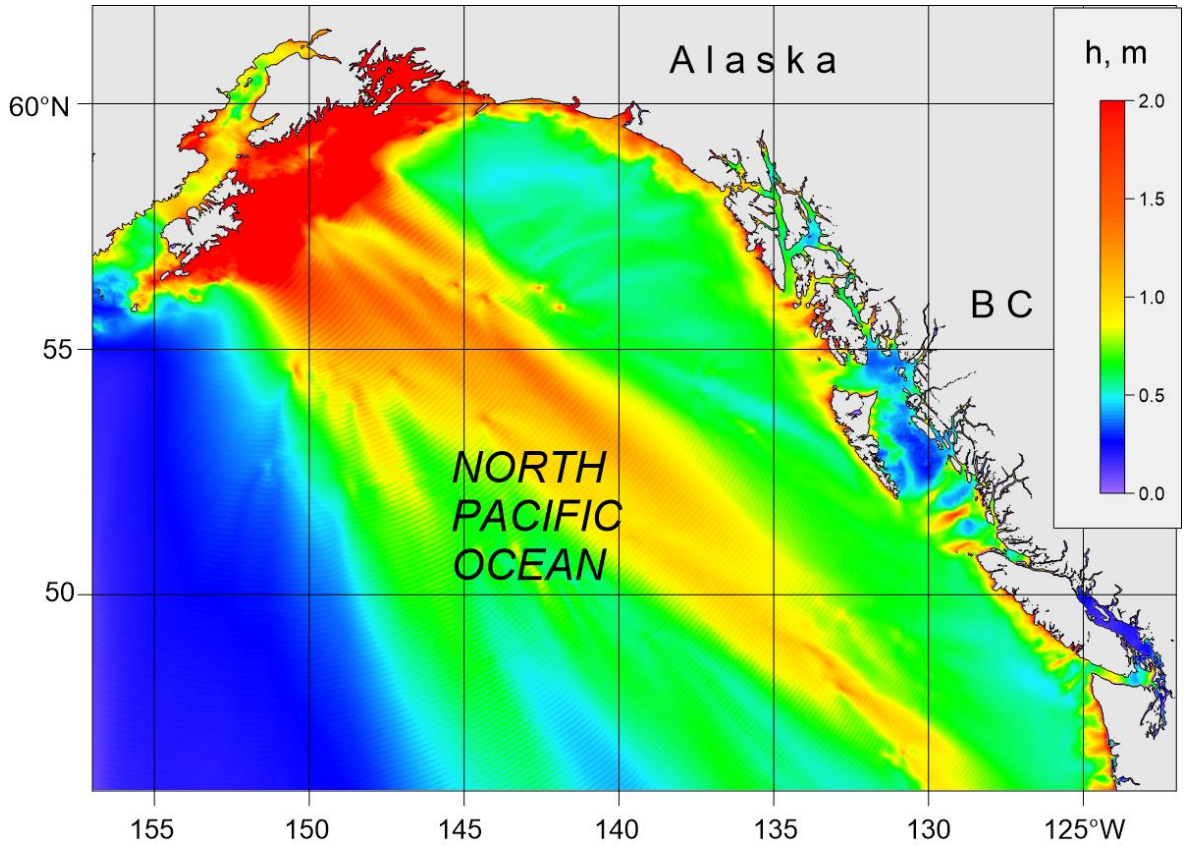

Figure 8. Distribution of maximum tsunami wave amplitudes (metres) for Grid 1 of the nested-grid model for waves generated by simulation of a 1964-type Alaska tsunami.

Results for the finer resolution grids (Grids 3-4) demonstrate the considerable spatial variability in the incoming tsunami wave amplitudes for the study region. Figure 10 shows the distribution of the tsunami wave amplitudes for Grid 3 in the southern Strait of Georgia off Metro Vancouver. As the figure indicates, the simulated wave amplitudes are much higher in Boundary Bay than along the coast of Metro Vancouver to the north. Waves increase toward the shoreline and are especially high in the upper part of Boundary Bay and in Drayton Harbor (see Figure 4 for the location). The pronounced increase in tsunami wave displacements in the harbour is related to resonance amplification of the incoming tsunami waves.

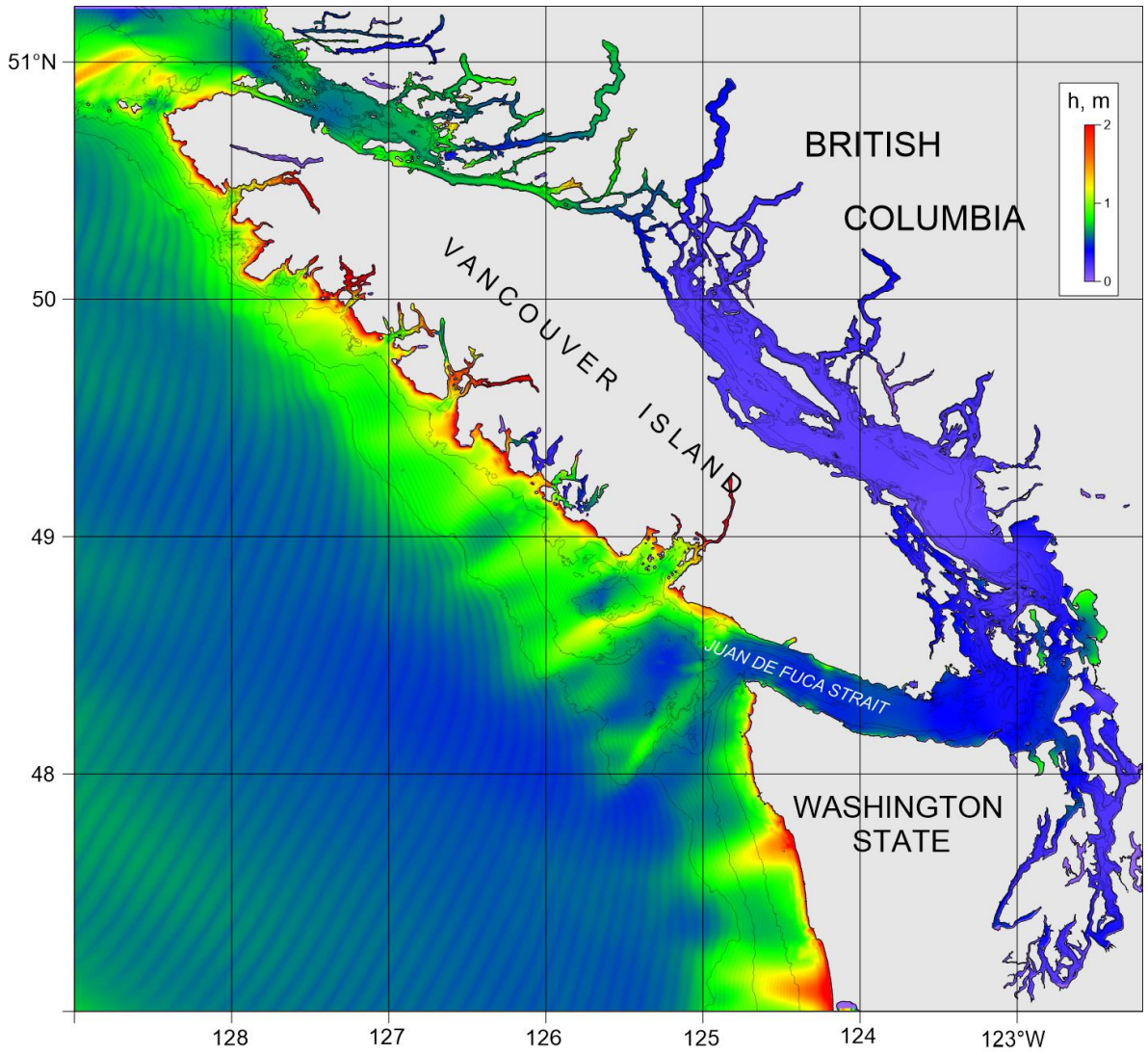

Figure 9. Distribution of maximum tsunami wave amplitudes (metres) for Grid 2 of the nested-grid model for waves generated by simulation of a 1964-type Alaska tsunami.

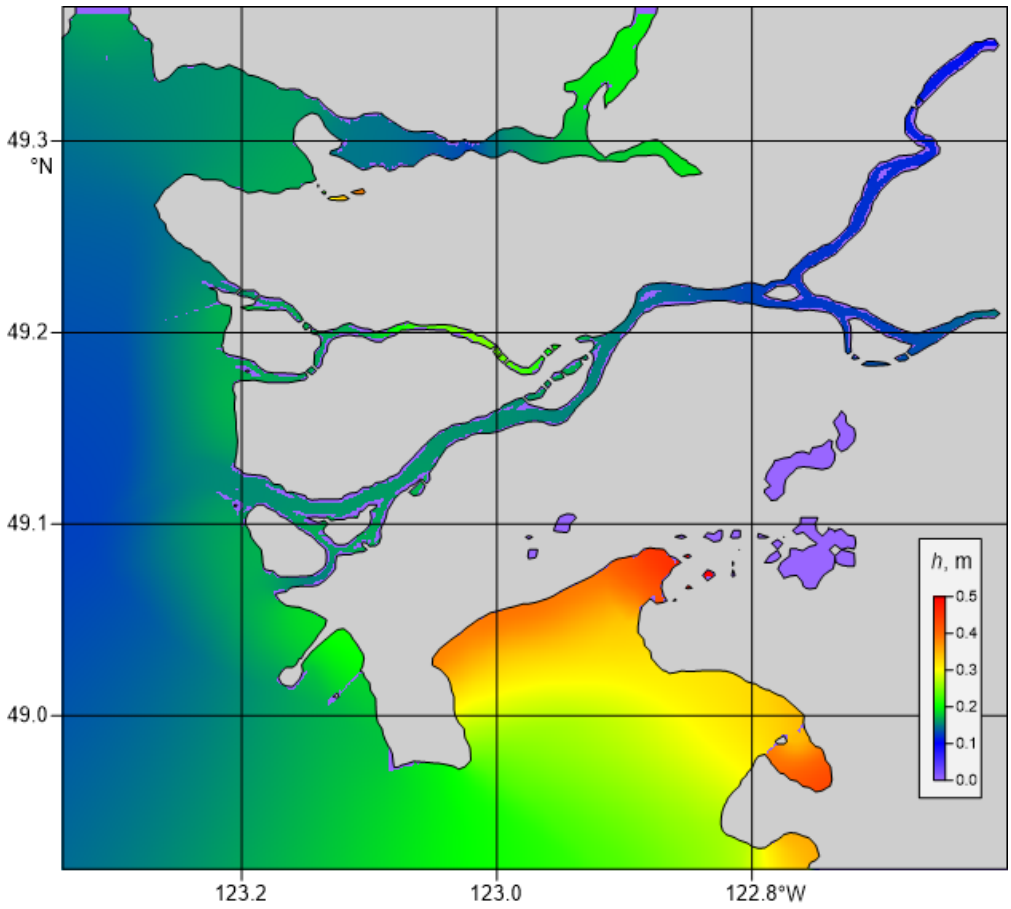

Figure 10. Distribution of maximum tsunami wave amplitudes (metres) for Grid 3 of the nested-grid model for waves generated by simulation of a 1964-type Alaska tsunami.

3.3. DETAILED RESULTS FOR BOUNDARY BAY: VARIATIONS OF SEA LEVELS AND TSUNAMI-INDUCED CURRENTS

Figure 11 presents a high-resolution map showing the distribution of the maximum tsunami amplitudes in Boundary Bay and vicinity. We note that the amplitudes of the tsunami waves gradually increase from the entrance to the head of the bay are almost to twice as high (0.40 m) as those at the entrance (~0.25 m). Another "hot spot" is Drayton Harbor, located at the south-east end of the grid, where wave amplitudes will reach 0.45 m. Figure 12 shows an enlarged (zoomed) version of the wave amplitude distribution for the Semiahmoo coast. It is clear that wave amplitudes are distributed uniformly along the coast, with values are 0.32-0.34 m.

Figure 13 presents the distribution of the tsunami-induced current maxima derived from the model. In most places, the current is weak and does not exceed 0.3 cm/s; however, the currents

induced at the entrance to Drayton Harbor reach 1.5 m/s (3 knots). The current at the Semiahmoo coast (Figure 14) is generally very weak, with the exception of the Campbell River mouth, where it can reach 1 m/s (2 knots).

Detailed analyses of the sea level variability and current speeds were carried out for 12 sites around Boundary Bay and Semiahmoo Bay (Figures 15-19; Tables 3-4).

The travel time to Boundary Bay from the Alaska 1964 source is around 5 hours, and the first, highest wave peak is reached 6 hours after the earthquake. Tsunami waves arrive first at Sites 9, 10, and 11, located on the Semiahmoo coast, then Sites 8, 7 and, finally, Site 1, approximately half an hour after the first waves arrive at the Semiahmoo coast. The lead wave is the highest, followed by the second wave, which is only marginally lower. The subsequent waves are lower than the first two waves.

Generally, it is evident that waves from an Alaska 1964-type tsunami at Boundary Bay are weak, and not a threat to the coastal communities. However, the tsunami creates a moderate wave-induced current at the entrance to Drayton Harbor, which could be dangerous for small boats.

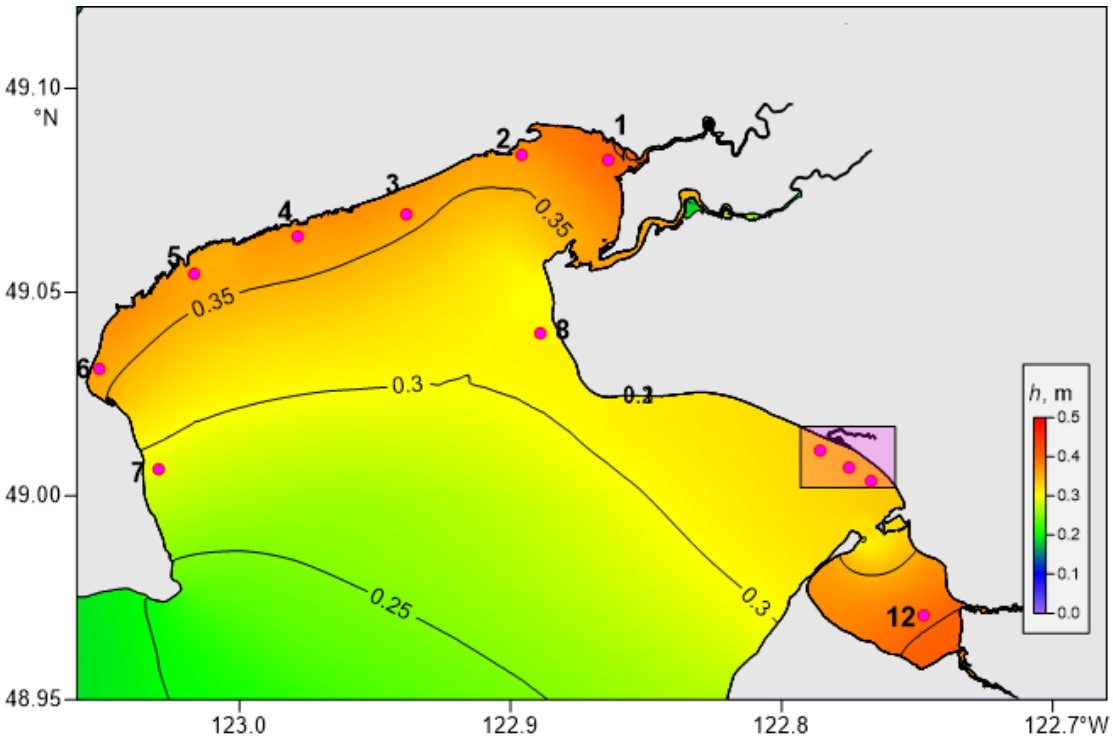

Figure 11. Distribution of maximum tsunami wave amplitudes (metres) for Grid 4 of the nested-grid model for waves generated by simulation of a 1964-type Alaska tsunami. Numbers in Boundary Bay denote sites for which tsunami wave records have been simulated.

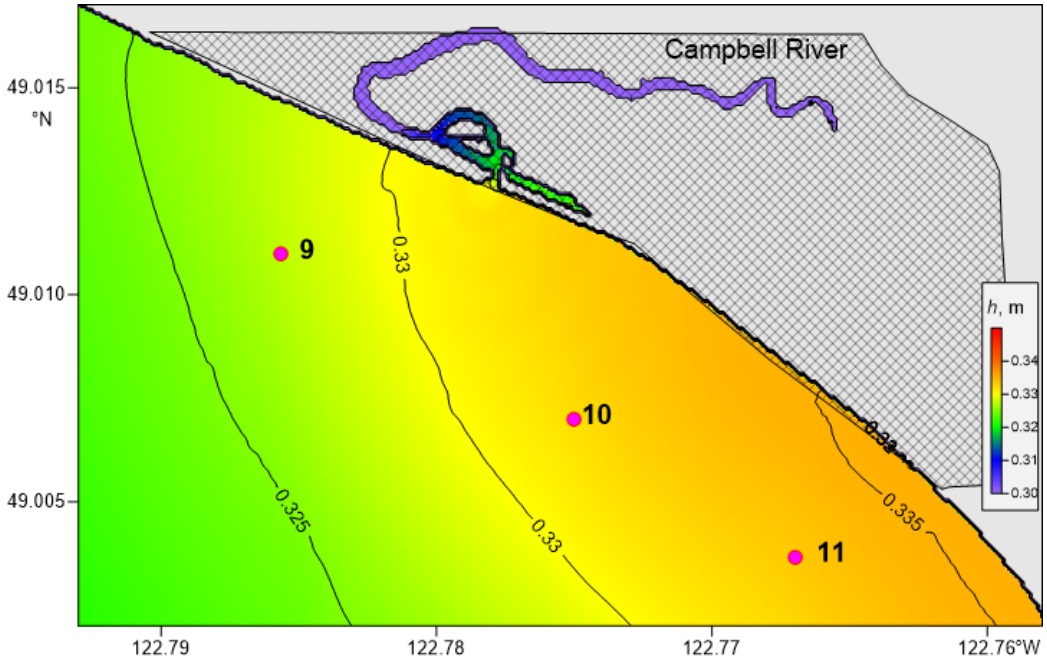

Figure 12. Distribution of maximum Alaska 1964-type tsunami wave amplitudes (*h*, m) on the Semiahmoo coast. Numbers denote sites for which tsunami wave records have been simulated

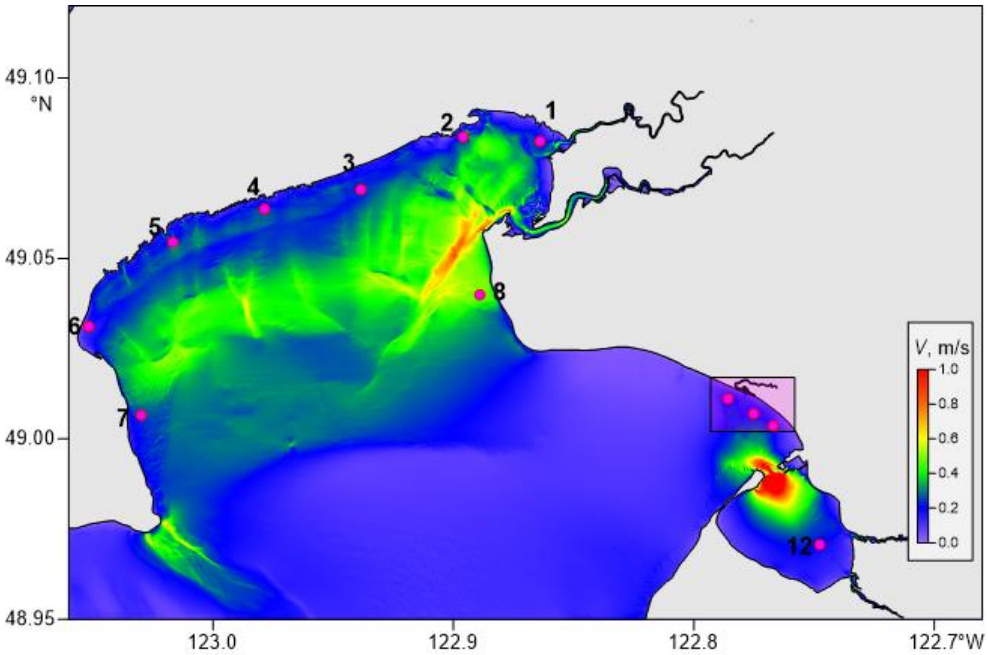

Figure 13. Distribution of the maximum Alaska 1964-type tsunami-induced current (*V*, m/s) for Grid 4 in Boundary Bay. Numbers denote sites for which tsunami wave records have been simulated.

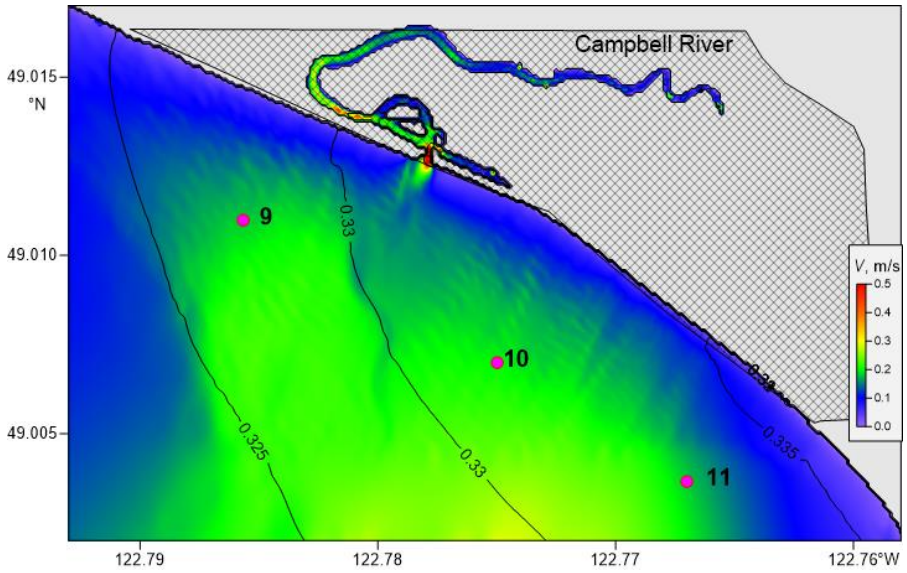

Figure 14. Distribution of the maximum Alaska 1964-type tsunami-induced current (*V*, m/s) for the Semiahmoo coast. Numbers denote sites for which tsunami wave records have been simulated.

Table 3. Tsunami wave parameters for a 1964-type Alaska tsunami at Boundary Bay for numerical simulations. See Figures 13-14 for the site locations. Travel times for the maximum waves are in hours and minutes (HH:MM) after the start of the earthquake. Wave displacements are measured relative to the still water level at the time of the event.

Site No	Highest crest		Deepest trough	
	Displacement (m)	Travel time HH:MM	Displacement (m)	Travel time HH:MM
1	0.40	6:22	-0.33	7:27
2	0.37	6:17	-0.33	7:18
3	0.36	6:10	-0.31	7:03
4	0.37	6:13	-0.18	7:22
5	0.35	6:13	-0.18	12:16
6	0.36	6:07	-0.35	6:57
7	0.29	5:57	-0.26	6:41
8	0.30	5:58	-0.27	7:01
9	0.33	5:54	-0.26	10:11
10	0.33	5:55	-0.27	10:12
11	0.33	5:56	-0.28	7:06
12	0.39	6:11	-0.32	7:15

Table 4. Wave-induced current speeds (*V*) for the numerical simulations of a Alaska 1964-type tsunami in Boundary Bay. See Figures 13-14 for the site locations. The times for the occurrence of maximum wave-induced currents are in hours and minutes (HH:MM) after the start of the earthquake.

Site No	Maximum current speed (m/s)	Time of maximum current speed HH:MM
1	0.22	7:54
2	0.20	7:53
3	0.24	7:41
4	0.26	10:53
5	0.32	6:39
6	0.15	10:43
7	0.26	6:17
8	0.48	6:32
9	0.18	6:15
10	0.20	6:19
11	0.18	6:43
12	0.20	10:20

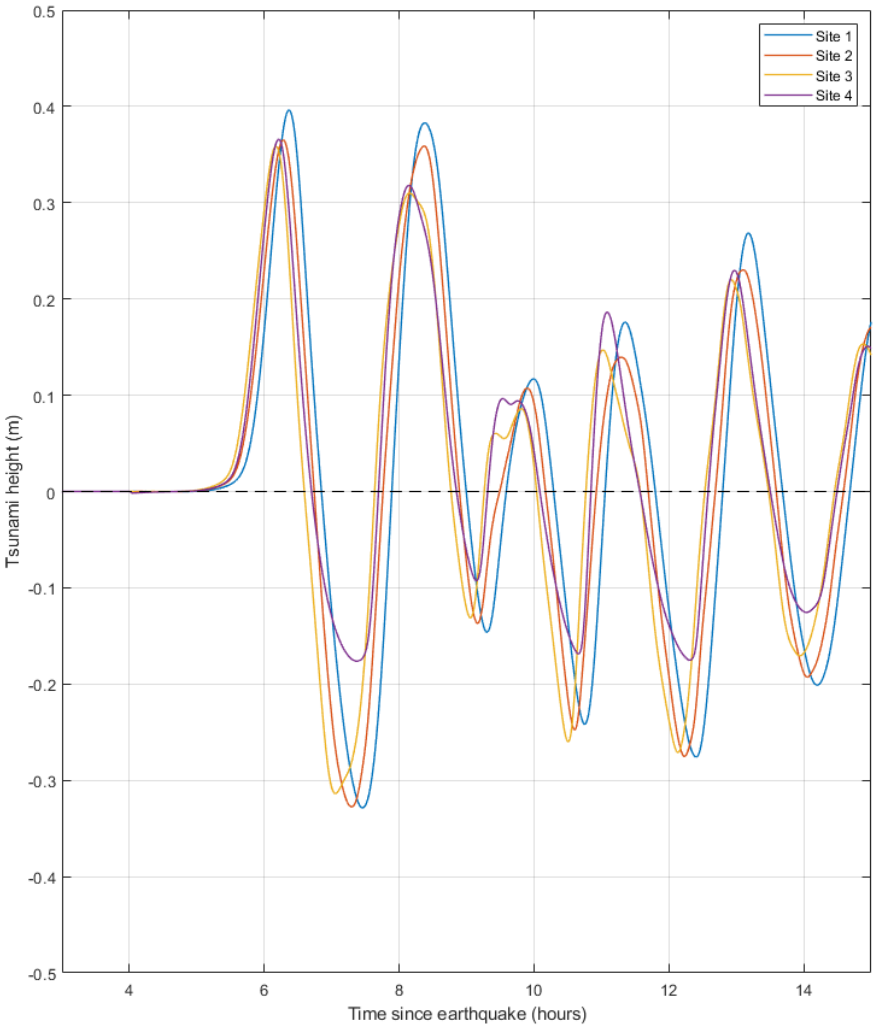

Figure 15. Simulated records of sea level variation for an Alaska 1964-type tsunami at Sites 1, 2, 3 and 4 (See Figure 13-14 for the site locations).

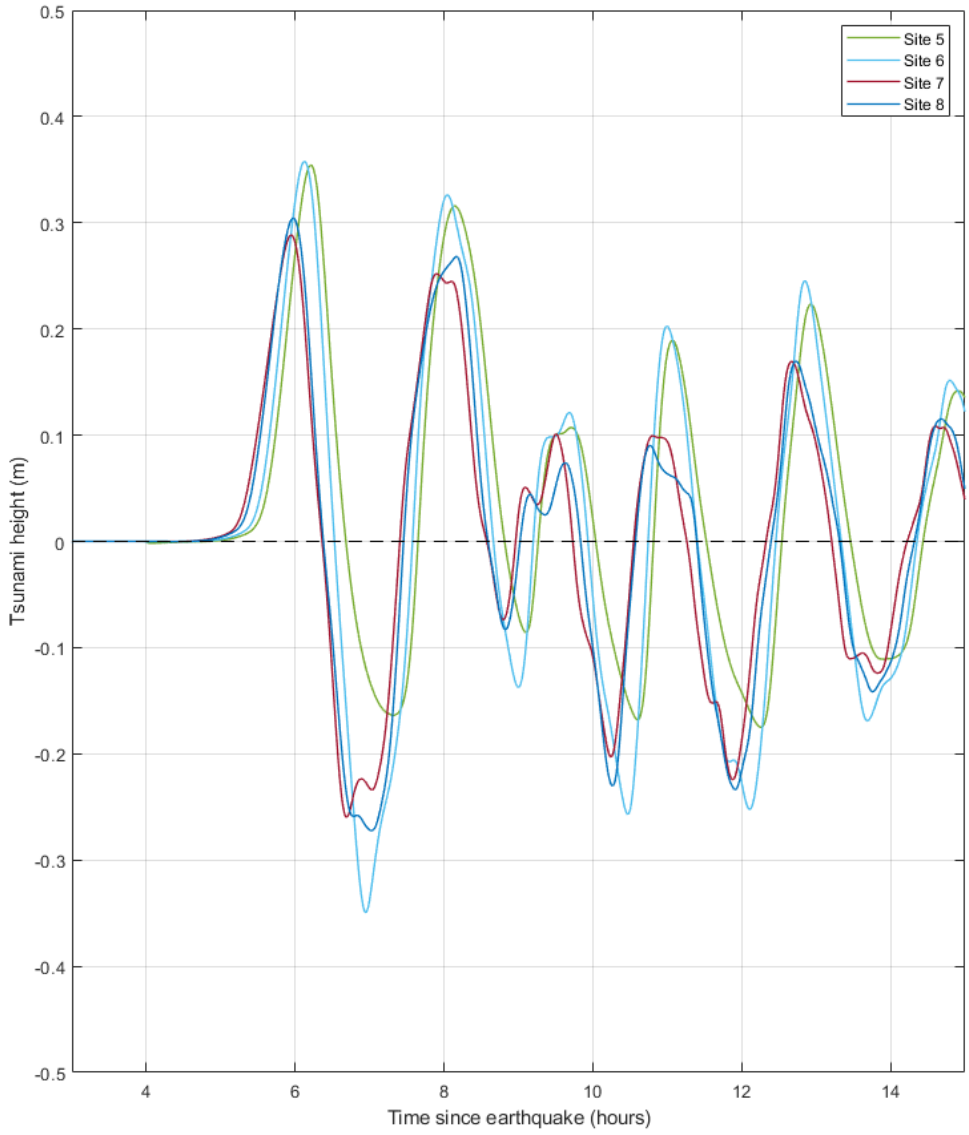

Figure 16. Simulated records of sea level variation for an Alaska 1964-type tsunami at Sites 5, 6, 7 and 8 (See Figure 13-14 for the site locations).

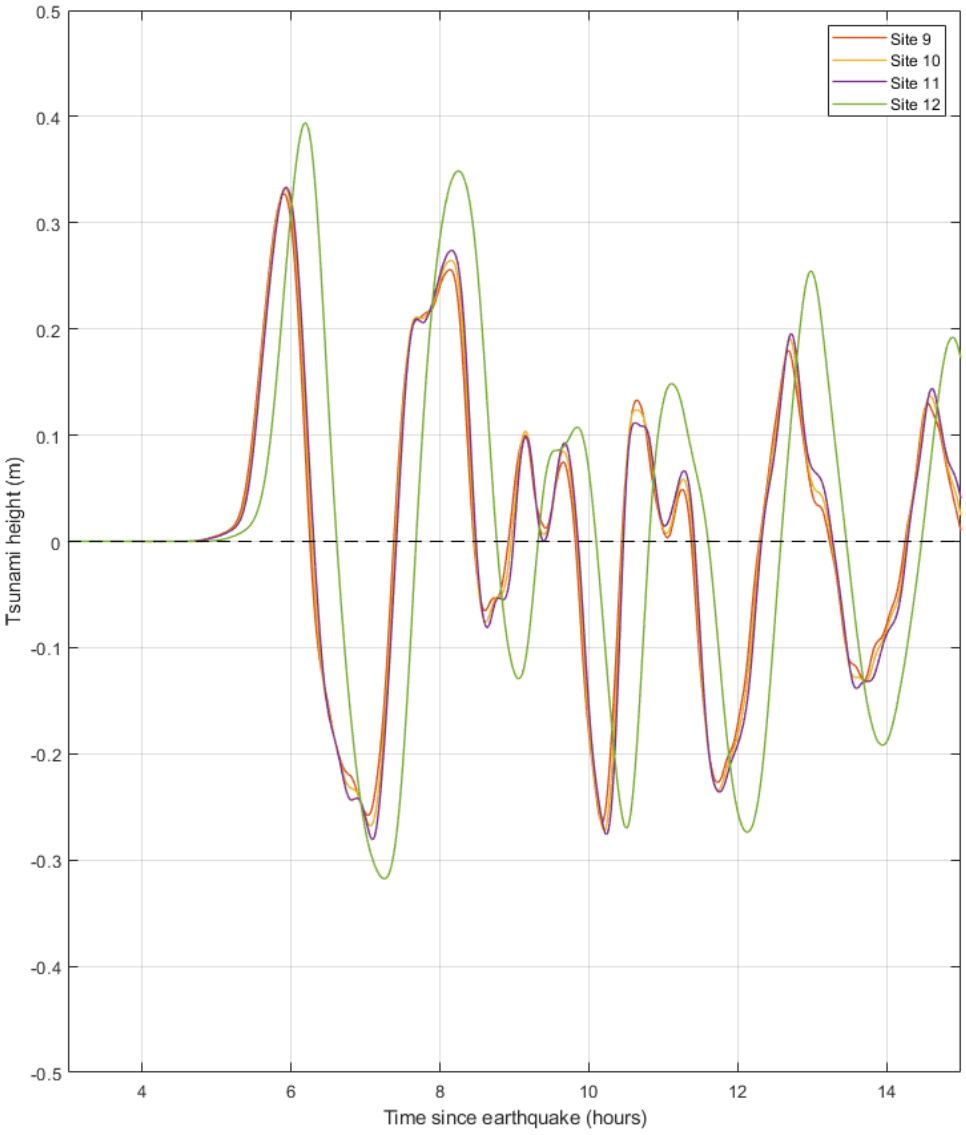

Figure 17. Simulated records of sea level variation for anAlaska 1964-type tsunami at Sites 5, 6, 7 and 8 (See Figure 13-14 for the site locations).

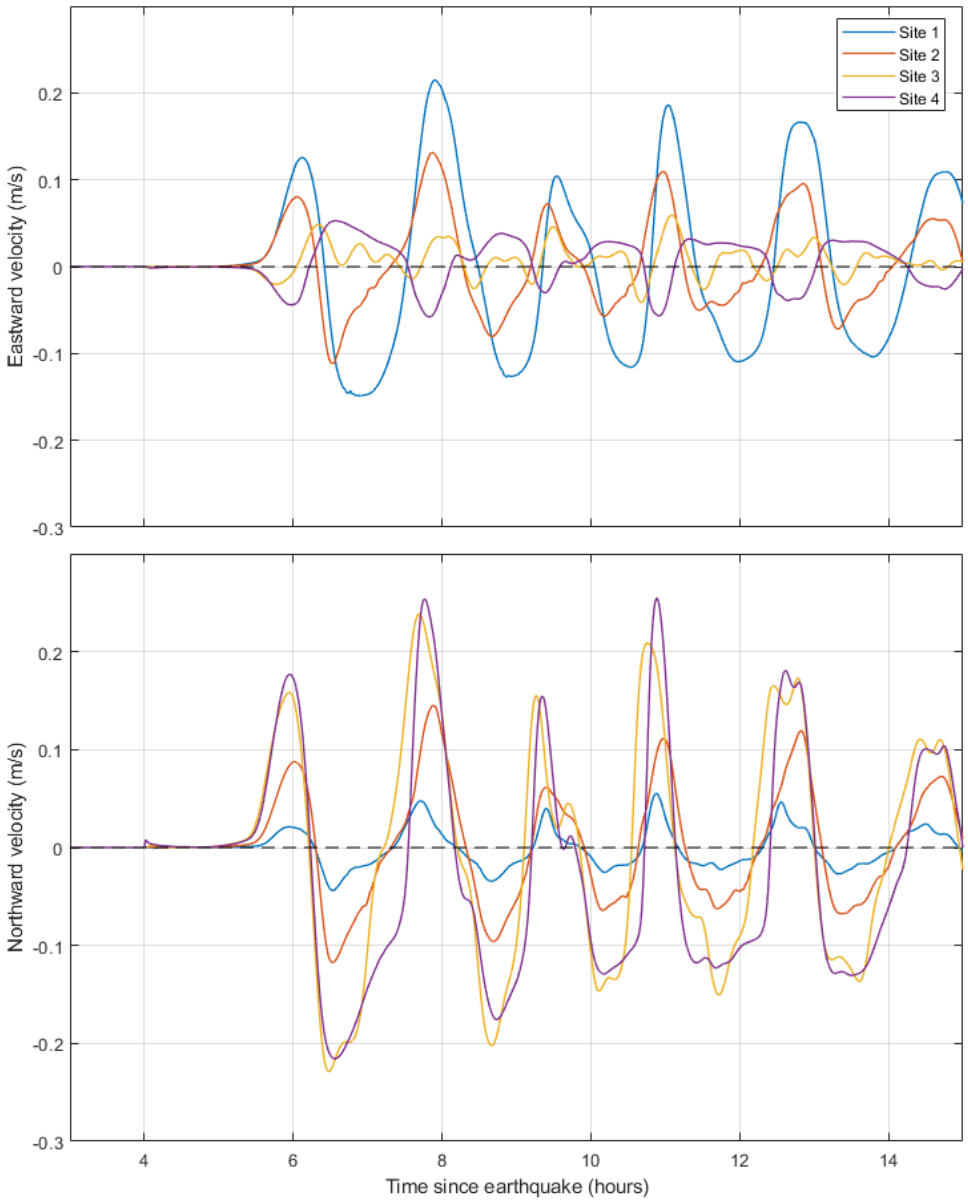

Figure 18. Simulated records of the eastward component of current velocity for an Alaska 1964-type tsunami at Sites 1, 2, 3 and 4 (See Figure 11 for the site locations).

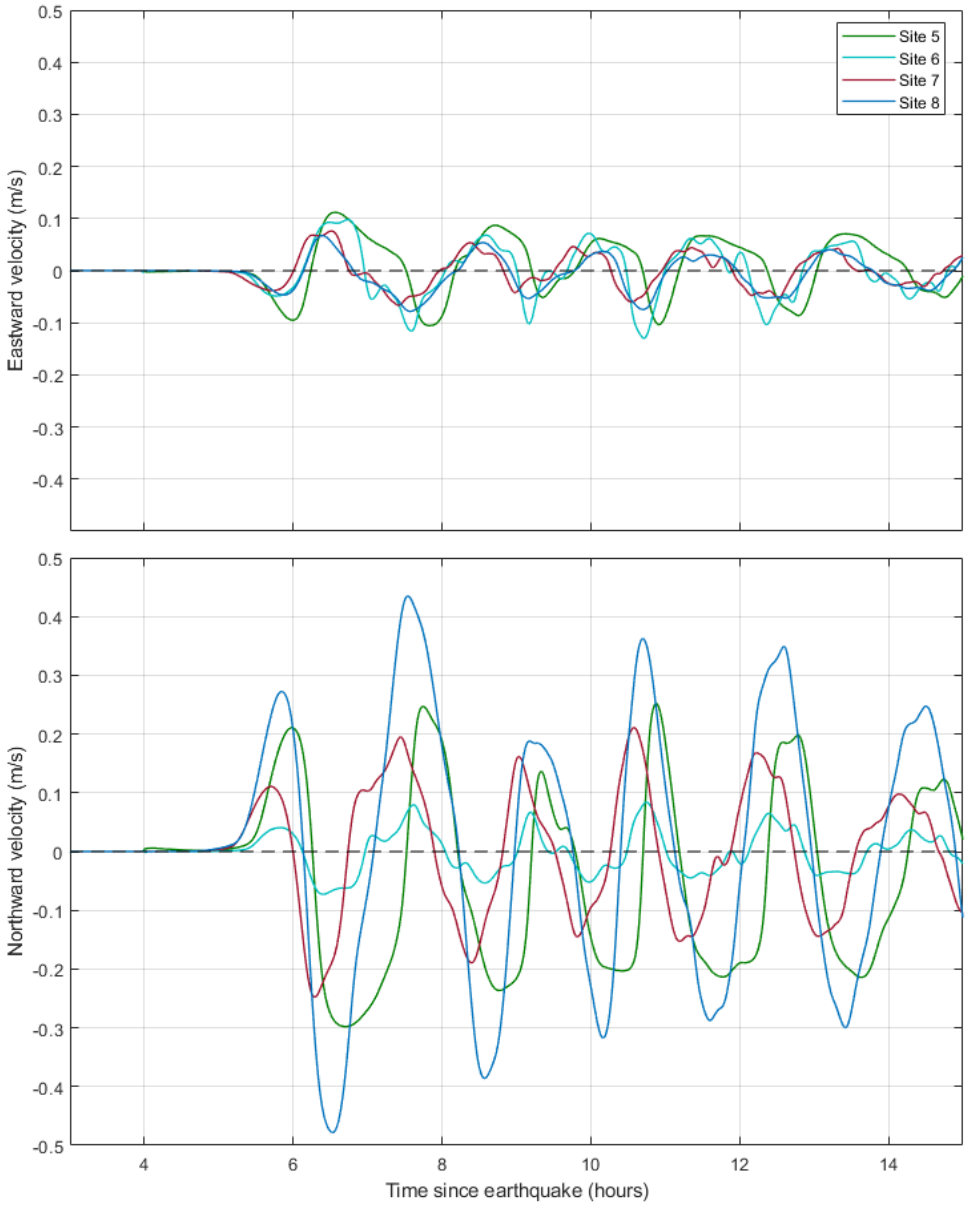

Figure 19. Simulated records of the northward component of current velocity for an Alaska 1964-type tsunami at Sites 1, 2, 3 and 4 (See Figure 13-14 for the site locations).

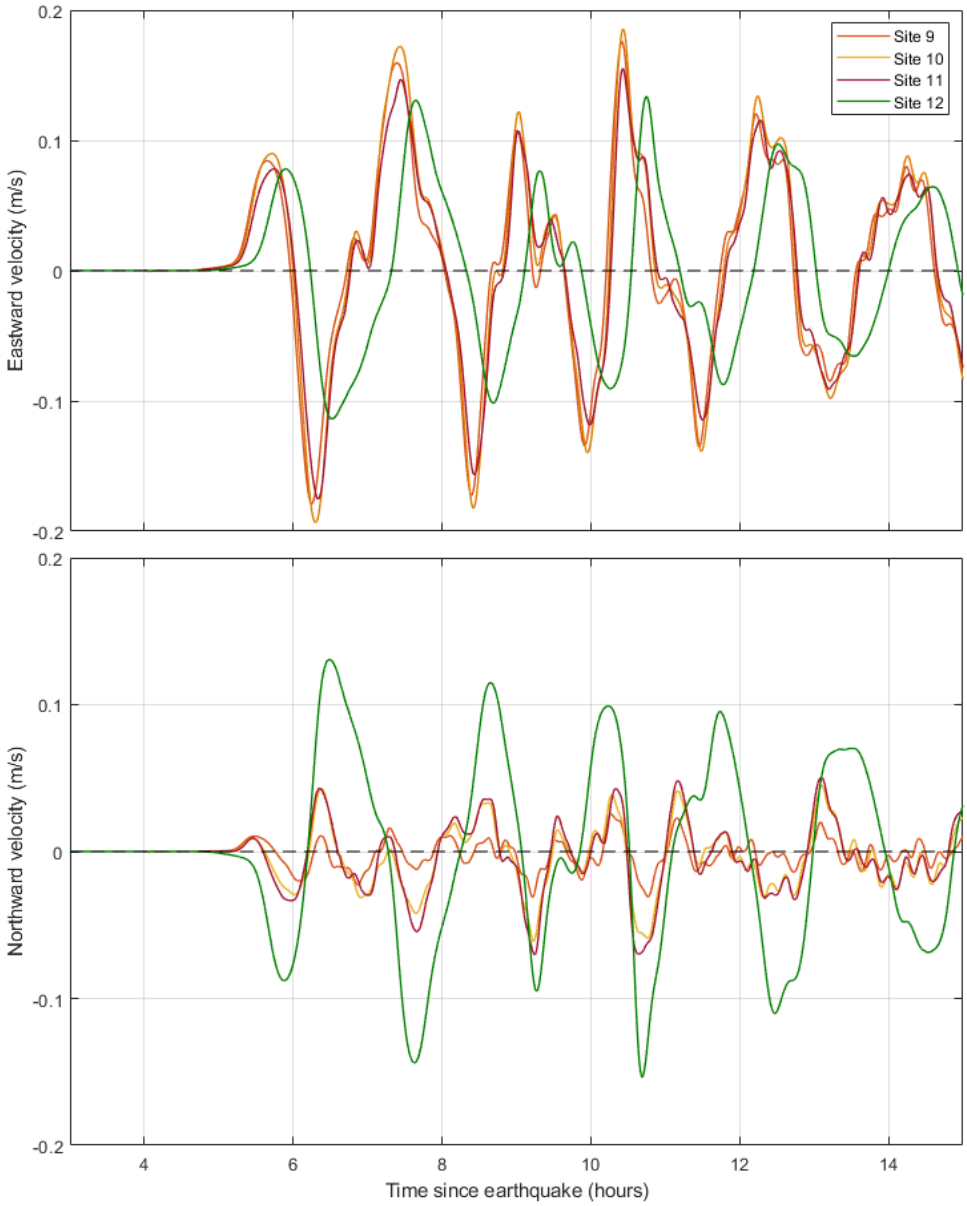

Figure 20. Simulated records of the eastward component of current velocity for an Alaska 1964-type tsunami at Sites 5, 6, 7 and 8 (See Figure 13-14 for the site locations).

4. CONCLUSIONS

A high-resolution, nested-grid tsunami model has been used to simulate the distribution of tsunami waves and wave-induced currents that will be generated in Boundary Bay in the event of a 1964-type Alaska tsunami. The model uses an advanced tsunami source distribution and high-resolution bathymetry for the area of interest. The major results of the modelling are:

- The tsunami in Boundary Bay will reach 0.45 m above the tidal level at the time of the wave arrivals, with the first wave being the highest wave; tsunami waves along the coast of Semiahmoo Bay will be up to 0.35 m.
- The distribution of tsunami wave amplitudes within Boundary Bay will be non-uniform, with highest waves occurring toward the head of the bay. The distribution of the wave amplitudes along the Semiahmoo coast will be nearly uniform.
- The tsunami will induce moderate currents at the entrance to Drayton Harbor (up to 1.5 m/s) and at the mouth of Campbell River (up to 0.5 m/s). At other locations, wave-induced current will not exceed 0.3 m/s.

Because details of future possible tsunamis remain unknown in many aspects, we recommend the use of a safety factor of 50%, which should be added to the tsunami amplitudes estimated for a 1964-type event. However, even with such a factor, the risk of flooding in Boundary Bay by an Alaska 1964-type tsunami, is low.

ACKNOWLEDGEMENTS

This project was funded through “Coastal Flood Mitigation Canada” within the Defence Research and Development Canada’s Centre for Security Science (DRDC CSS) Program (CSSP), led on the Pacific Coast by the Geological Survey of Canada, Natural Resources Canada. We thank Marlene Jeffries (Canadian Hydrographic Service) and Mark Ranking (Ocean Networks, Canada) for providing us with the high-resolution bathymetric and topographic data for the Boundary Bay region and for helping with the vertical datum adjustment. The authors gratefully thank Elena Suleimani (University of Alaska at Fairbanks) for providing us the latest source model for the Alaska 1964-type earthquake and tsunami and Maxim Krassovski (Insititute of Ocean Sciences, DFO) for providing a digital record of the Alaska 1964 tsunami at Point Atkinson.

REFERENCES

Anderson, P. S. and Gow, G. A. (2004), *Tsunamis and Coastal Communities in British Columbia: An Assessment of the B.C. Tsunami Warning System and Related Risk Reduction Practices.*75xii pp. (Public Safety and Emergency Preparedness Canada, Ottawa, 2004)

British Columbia 3 arc-second Bathymetric Digital Elevation Model (2017). https://www.ngdc.noaa.gov/metaview/page?xml=NOAA/NESDIS/NGDC/MGG/DEM/iso/xml/4956.xml&view=getDataView&header=none

Clague, J.J., Munro, A., and Murty, T.S. (2003), Tsunami hazard and risk in Canada, *Natural Hazards* 28 (2-3), 433-461.

Dunbar, D., LeBlond, P., and Murty, T.S. (1991). Evaluation of tsunami amplitudes for the Pacific coast of Canada. *Progress in Oceanography*, 26, 115-177.

Fine, I.V., Cherniawsky, J.Y., Rabinovich, A.B., and Stephenson, F.E. (2008), Numerical modeling and observations of tsunami waves in Alberni Inlet and Barkley Sound, British Columbia, *Pure and Applied Geophysics*, 165 (11/12), 2019-2044.

Fine, I.V., Thomson, R.E., Lupton, L.M. and Mundschutz, S. (2018a.), *Numerical Modelling of an Alaska 1964-type Tsunami at the Canadian Coast Guard Base in Victoria, British Columbia*. Can. Tech. Rep. Hydrogr. Ocean Sci. 323: v + 28p.

Fine I.V., Thomson, R.E., Lupton, L.M., and Mundschutz, S. (2018b). *Numerical modelling of a Cascadia subduction zone tsunami at the Canadian Coastal Base at Victoria, British Columbia*, Can. Tech. Rep. Hydrogr. Ocean Sci. 324: v + 30p.

GEBCO One Minute Grid, The. Version 2.0 (2014), http://www.gebco.net.

Imamura, F., Shuto, N., and Goto, C. (1988). Numerical simulation of the transoceanic propagation of tsunamis. Paper presented at the Sixth Congress of the Asian and Pacific Regional Division. *Int. Assoc. Hydraul. Res*., Kyoto, Japan. vol.IV, p. 265-272.

Imamura, F., Yalciner, A.C., and Ozyurt, G. (2006). *Tsunami Modelling Manual* (TUNAMI Model), 2006. http://www.tsunami.civil.tohoku.ac.jp/hokusai3/J/projects/manual-ver-3.1.pdf

Johnson, J.M., Satake, K., Holdahl, S.R., and Sauber, J. (1996). The 1964 Prince William Sound earthquake— Joint inversion of tsunami waveforms and geodetic data. *Journal of Geophysical Research*, 101 (B1), 523–532.

Lander, J.F. (1996). *Tsunamis Affecting Alaska, 1737-1996*. Boulder, CO: U.S. Department of Commerce.

Liu, P. L.-F., Woo, S-B., and Cho, Y-S. (1998). *Computer Programs for Tsunami Propagation and Inundation*. Technical report, Cornell University.

Matheron, G. (1963). *Principles of Geostatistics*. Economic Geology, 58, pp 1246–1266.

Myers, E.P. and Baptista, A.M. (2001), Analysis of factors influencing simulations of the 1993 Hokkaido Nansei-Oki and 1964 Alaska tsunamis. *Natural Hazards*, 23, 1-28. https://doi.org/10.1023/A:1008150210289

NOAA (2017). *British Columbia, 3 arc-second MSL DEM*. https://www.ngdc.noaa.gov/dem/squareCellGrid/download/4956. Last access on 11.10.2017.

National Tsunami Hazard Mapping Program (NTHMP) (2010). *Guidelines and best practices for tsunami inundation modeling for evacuation planning*. NTHMP Mapping & Modeling Subcommittee, NOAA, USA.

Nikolsky, D.J., Suleimani, E.N., Haeusseller, P.J., Ryan, H.F., Kohler, R.D., Combellick, R.A., and Hansen, R.A. (2013). *Tsunami Inundation maps of Port Valdez, Alaska*. State of Alaska, Department of Natural Resources, Division of Geological & Geophysical Surveys.

Spaeth, M.G. and Berkman, S.C. (1967). *The Tsunami of March 28, 1964, as Recorded at Tide Stations.* Coast and Geod. Survey Techn. Bull. 33, US Department of Commerce, 86 p.

Suito, H. and Freymueller, J.T. (2009). A viscoelastic and afterslip post seismic model for the 1964 Alaska earthquake. *Journal of Geophysical Research,* 114 (B11404), doi:10.1029/2008JB005954.

Suleimani, E.N. (2011). *Numerical Studies of Tectonic and Landslide-Generated Tsunamis Caused by the 1964 Great Alaska Earthquake*. Fairbanks, Alaska, University of Alaska Fairbanks, Ph.D. dissertation, 181 p.

Suleimani, E.N., Nicolsky, D.J., and Koehler, R.D. (2013). *Tsunami Inundation Maps of Sitka, Alaska.* Report of Investigations 2013-3, State of Alaska, Department of Natural Resources, Division of Geological and Geophysical Surveys, Fairbanks, AK, 76 p., 1 sheet, scale 1:250,000. doi: 10.14509/26671.

Thomson, R.E. and Emery, W.J. (2014). *Data Analysis Methods in Physical Oceanography: 3rd Edition.* Elsevier Science, Amsterdam, London, New York (August 2014), 716 p.

Wang, X. (2009). *User Manual for COMCOT Version 1.7*. http://ceeserver.cee.cornell.edu/pll-group/doc/COMCOT_User_Manual_v1_7.pdf.